CLOUD PROPERTIES DERIVED FROM AVHRR DATA

K.-T. Kriebel
Deutsche Forschungsanstalt für Luft- und Raumfahrt
Oberpfaffenhofen, FRG

1. INTRODUCTION

From the beginning of the NOAA-TIROS-N satellite series it was tried to use the spectral information of the 'Advanced Very High Resolution Radiometer ' (AVHRR) which is nearly twice that of the imagers onboard the geostationary satellites, to improve the cloud classification (Liljas, 1984; Arking and Childs, 1985). To obtain high quality sea surface temperatures, algorithms to identify cloudy pixels have been developed which make use of the temperature dependence of the Planck function at 3.7 μm and 12 μm (Saunders, 1986) as well as the spectral differences of the transmittance of thin clouds and fog (e.g. Eyre et al., 1984). Liljas (1988) has used spectral data, channel differences and homogeneity tests in various channels to extract 10 criteria which allow each pixel to be assigned to one of 22 classes. To account for seasonal, regional and temporal variability, he has used test areas for each class and each situation. This method is operational and very effective, however it has been validated so far only by conventional analysis, i.e. in a more statistical manner.

At the Robert Hooke Institute for Cooperative Atmospheric Research in Oxford, U.K., a somewhat different idea has been followed. In a first step, each pixel is classified into one of the three possible groups cloud-free, fully cloudy, and partially cloudy. Cloud classification and analysis starts after this cloud detection has been successfully completed (Saunders and Kriebel, 1988). This procedure is presented in the following. It is called 'AVHRR Processing scheme Over cLouds, Land and Ocean' and is abbreviated as APOLLO.

2. CLOUD DETECTION

The basic idea of the satellite data processing scheme presented here, is to use parameterized relations to obtain surface properties like albedo, surface temperature and vegetation index from cloud-free pixels, and cloud optical properties like optical depth, liquid or ice water path, emissivity and cloud top temperature from fully cloudy pixels. It is therefore essential for the quality of the products that only those pixels are called cloud-free where there is no doubt. The same is true for fully cloudy pixels vice versa. At first, each pixel is tested by up to five algorithms whether it is cloud contaminated or not. It is only called cloud-free, if none of the five algorithms says it is cloudy. Secondly, the group of cloud contaminated pixels is tested whether they are fully cloudy or not. The disadvantage of such a careful procedure is an overestimation of the partially cloudy pixels. Because this group is essential for the determination of the cloud coverage (the other two groups have only to be counted), the algorithms to determine the cloud coverage of partially cloudy pixels must allow for such an overestimation.

The choice of the algorithms was accomplished according to their simplicity together with an effective exploitation of the available spectral information. The 'Advanced Very High Resolution Radiometer' (AVHRR) is presently used in two versions. AVHRR/1 is

onboard NOAA 6, 8, 10 and has 4 spectral channels (the 5. channel duplicates the 4. channel). AVHRR/2 onboard NOAA 7, 9, 11 has a channel 5 different from channel 4. Channel 1 and 2 are centered in the visible and near infrared portion of the spectrum. They separate the part below 0.7 μm, where the reflectance of vegetation is low and water vapour does not absorb, from the part above 0.7 μm, were vegetation has a high reflectance and water vapour strongly absorbs (cf. Table 1). Channel 4 and 5 of the AVHRR/2 divide the atmospheric infrared window into two regions with different temperature dependence of the Planck function and different transmittance of thin clouds. Additionally, the water vapour absorption is different which can be used to correct for the atmospheric masking of the surface temperature. This 'split-window' information is the reason for the AVHRR is considered superior to the imaging radiometers of present geostationary satellites, which have only one broad channel in similar spectral bands. A special role plays channel 3 at 3.7 μm. Daytime data contain equivalent amounts of reflected and emitted radiations which cannot be separated without additional information. Channel 3 is therefore used mainly during nighttime where it contributes essentially to the cloud detection. During daytime it is used mainly to discriminate clouds from snow and ice.

NOAA		MSG	
AVHRR/2 [μm]	Kanal	VIRI [μm]	Kanal
0.58 - 0.68	1	0.60 - 0.67	VIS1
0.725 - 1.1	2	0.77 - 0.89	VIS2
		1.53 - 1.70	IR1.6
3.55 - 3.93	3	3.5 - 3.9	IR3.7
		5.8 - 6.7	WV1
		6.9 - 7.3	WV2
10.3 - 11.3	4	10.3 - 11.3	IR11
11.5 - 12.5	5	11.5 - 12.5	IR12

Table 1: Spectral channels of the 'Advanced Very High Resolution Radiometer' (AVHRR/2) onboard the TIROS-N/NOAA satellite series and the corresponding recommendations for the 'Visible and Infrared Imager' (VIRI) of the METEOSAT Second Generation satellite system (MSG).

The five algorithms used in APOLLO to detect cloud-free pixels consist of two threshold tests which are also in use with data from geostationary satellites, and of two 'split-window' tests which make use of the splitting of the solar and terrestrial spectral ranges. The fifth method uses spatial coherence to identify clouds. This can be looked at as a first step to pattern recognition techniques though it uses only horizontal variance to measure the inhomogeneity of the surface. Because this test is applied only over the ocean, it must additionally be known whether the pixel contains ocean or land surface (or coast). This is accomplished by means of a land-sea-mask which is built up for the area under consideration from a terrain data bank after the navigation has been successfully performed. Further, all spectral channels have to be calibrated because the algorithms require equivalent temperatures and reflectance factors instead of counts. Calibration is easily performed with channel 3, 4 and 5 by using of the calibration information included in the data stream. With channel 1 and 2 the preflight calibration has to be used (Lauritson et al., 1979). Recent investigations (Rao, 1987; Price, 1987; Brest and Rossow, 1988; Frouin and Gautier, 1987) are concerned with temporal changes of the calibration factors and show ways to account for such changes.

After having successfully identified cloud-free pixels, fully cloudy pixels are extracted from all the cloud contaminated pixels. To do so, two of the above mentioned five algorithms are applied again but only to those pixels not declared to be cloud-free and with a different interpretation. In the first round, the spatial coherence test has flagged all ocean pixels as not cloud-free whose 3 x 3 matrix of their surrounding has had a higher temperature variance than 0.25 K. Now knowing that all pixels are cloud contaminated, fully cloudy pixels are more homogeneous in cloud top temperature than are broken clouds. Because this is true over land as well as over the ocean, the pixel is called fully cloudy as long as the variance of its 3 x 3 temperature matrix is less than 1 K.

The second test is the ratio of the reflectance factors in channel 2 and 1. This relation is clearly larger than 1 over land surfaces, at least if vegetation is present. Over the clear ocean and outside the sunglint this relation is always less than 0.7 because the ocean reflectance is very low and the atmospheric backscattering has a mean wavelength dependence of λ^{-4} for molecules and $\lambda^{-1.3}$ for aerosols. Clouds, however, reflect nearly equal in both channels. Immediately above the cloud, the ratio is nearly equal to 1. On the way to the satellite the radiance is extincted by ozone in channel 1 and by water vapour in channel 2. This results in ratios of the reflectance factors larger than 1 for high clouds (up to about 1.1) and less than 1 for low clouds (down to 0.8). Hence, this ratio is a cloud height indicator, however a rather coarse one. To detect cloud-free pixels, the thresholds are set at 0.7 and 1.6 for moderate climates. All pixels with ratios larger than 0.7 over the ocean and less than 1.6 over land are flagged as not cloud-free. To detect fully cloudy pixels, a histogram is formed from the ratio values of the not cloud-free pixels and it is looked for a peak between 0.8 and 1.1. If there is a peak, it must be due to fully cloudy pixels. The area from which the histogram is formed contains 50 x 50 pixels, i.e. roughly 55km x 55km. All pixels whose ratio is inside the range of ± 0.05 from the peak value are flagged as fully cloudy. If no peak is found a default value of 0.9 is assumed. A detailed description of all the algorithms can be found in Saunders and Kriebel (1988).

Initially only those pixels have been called fully cloudy which have been flagged fully cloudy from both tests. It was found, however, that the yield of fully cloudy pixels became more realistic if also those pixels are called fully cloudy which are flagged fully cloudy by either of the two tests. Especially with convective clouds the spatial coherence test fails frequently whereas the ratio test gives good results. With thin clouds, on the contrary, the spatial coherence test is correct and the ratio test fails because the ratio is dominated by radiation reflected at the surface.

What has been said so far requires that there is neither snow nor ice. This is certainly true in many areas during the summer period. If there is snow or ice, however, the combination of algorithms presented so far fails because snow and ice pixels are flagged not cloud-free because of their high reflectance and are very likely flagged as fully cloudy. A solution is offered by the use of channel 3 at 3.7 μm (cf. Raschke et al., 1987). In this spectral range the reflectance of water clouds, ice clouds and snow is different (Welch et al., 1980). However these differences are unique only if the thermally emitted radiance is known. The temperature is known from channel 4, but the emissivity in channel 3 is widely unknown. It could be measured from nighttime data but nearly no data are presently available. Therefore the assumption of zero transmittance in this spectral region is required which is true for the surface and for thick clouds but not for thin clouds. With this assumption reflectance = 1 - emittance and the unknown emittance can be omitted from the equation for the reflectance (Ruff and Gruber, 1983). Together with other tests

like, e.g., the difference of channel 1 and 2 reflectance, two empirical thresholds now determine whether it is snow, ice or cloud or combinations of them (Gesell, 1989).

3. CLOUD CLASSIFICATION

Cloud detection is finished if all pixels of an AVHRR scene are put into one of the three boxes cloud-free, fully cloudy and partially cloudy. Now cloud classification consists of the task to assign each cloudy pixel to one atmospheric layer according to its cloud top temperature and the actual temperature profile. Because the latter is usually not known, only three height levels and ice clouds (cold and dark) are presently distincted in APOLLO (low > 700 hPa > medium > 400 hPa > high clouds). In this matter the Stockholm algorithm is presently much more differentiated (Liljas, 1988) because it allows for 16 different cloud classes. If not only the fully cloudy but also the partially cloudy pixels shall be assigned to a certain category, as is necessary, e.g., to determine the cloud coverage for each cloud type, an assumption of horizontal homogeneity is required saying that the clouds inside the partially cloudy pixel are of the same height as those of the nearest fully cloudy pixel. From this a unique assignment of the cloud type follows as well as the possibility to determine the cloud coverage of the partially cloudy pixel. Additionally, knowledge of the reflectance factors or the surface temperature of the partially cloudy pixel is required. Those can be obtained either from a terrain data bank, e.g. built up from previous cloud-free situations together with a forecast for the actual situation, or from the nearest cloud-free pixel.

The cloud coverage N of a partially cloudy pixel can be obtained either from the emitted radiance or from the reflectance factors:

$$L_m = (1-N)\,L_s + NL_c \quad \succ \quad N = \frac{L_s - L_m}{L_s - L_c}$$

with $L_m = \int \Phi_4(\lambda)\varepsilon(\lambda)\,B_\lambda(T)d\lambda$ = measured radiance, $\Phi_4(\lambda)$ = spectral sensitivity of channel 4, $\varepsilon(\lambda)$ = spectral emissivity, $B_\lambda(T)$ = Planck's function, L_s = radiance of the cloud-free surface, L_c = radiance at cloud coverage N = 1;

$$R_{1m} = (1-N)\,R_{1s} + NR_{1c}$$

$$R_{2m} = (1-N)\,R_{2s} + NR_{2c} \quad \succ \quad N = 1 - \frac{R_{2m} - QR_{1m}}{R_{2s} - QR_{1s}}$$

$$Q = R_{2c}/R_{1c}$$

with R_{1m}, R_{2m} = measured reflectance factors in the channel 1 and 2, R_{1s}, R_{2s} = reflectance factors of the cloud-free surface, R_{1c}, R_{2c} = reflectance of the clouds, Q = peak of the histogramm made from ratio values of R_{2c}/R_{1c} in an area of about 50 x 50 pixels containing the pixel under consideration.

In Figure 1, cloud coverages obtained from both techniques are shown. Though the scatter is large, the average values are close to the 45 ° line. Therefore the result should be independent from the method applied.

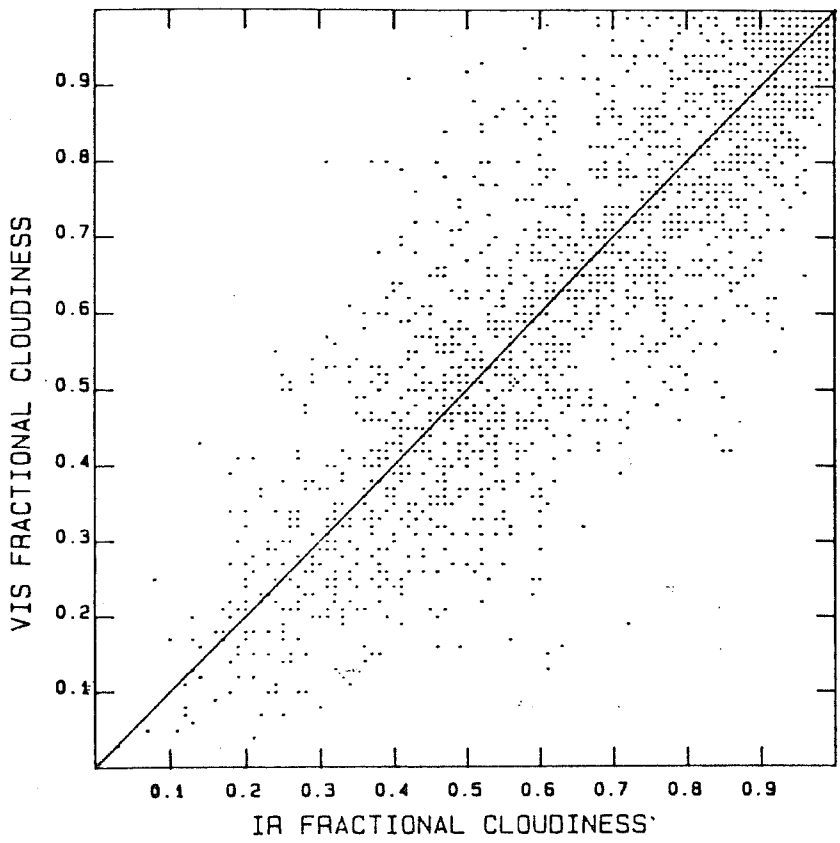

Figure 1: Cloud coverages of partially cloudy pixels obtained from both the emitted radiances (abscissa) and the reflectances (ordinate).

4. CLOUD ANALYSIS

Cloud analysis is understood to quantitatively relate spectral radiances of the AVHRR channels to cloud optical properties. It usually requires fully cloudy pixels to avoid interference with lower level or surface radiance. The parameter most frequently used is the cloud top temperature. It follows immediately from the measured radiance, e.g. in channel 4, by inversion of Planck's function. A correction is required which accounts for the atmosphere above the cloud (Saunders, 1988). From model computations, Stephens (1978) has derived a unique relation between the liquid water path and the optical depth of water clouds. The variability due to different droplet size distributions results in a $\pm$ 10 % uncertainty of this relation. A similar result was obtained for the relation between emissivity and liquid water path. The purpose of Stephen's parameterization was to conclude from measured data of the liquid water path (the vertical integral over the liquid water content) to changes in the radiation budget by means of a simple relation between optical depth and cloud reflectance which he has modified to hold for thick water clouds also. Kriebel (1989) follows this idea upside down and concludes from cloud reflectance to optical depth, liquid water path and emissivity by using Stephen's parameterization in the opposite direction. A major step in this procedure is the conversion of measured radiance or the measured bidirectional reflectance factor at the top of the atmosphere into the directional-hemispherical reflectance of the cloud. With ice clouds the parameterization is somewhat more complicated. On the one hand there is a correction factor

given by Platt et al. (1980), which accounts for the higher reflectance of an ice cloud compared to a water cloud at equal optical depth. This correction factor is presently not very well known. Another parameterization was published by Starr and Cox (1985). It relates the reflectance with the emissivity and, further, with the ice water path. Because it relies on the reflectance averaged over the spectral range 0.3-3 μm, a correction is applied according to the ratio of the reflectances at 0.55 μm and of the averaged reflectance. After Welch (1980), this correction factor is 1.14. In the following the rather simple formalism is presented.

Starting point is the measured reflectance in channel 1, because water vapour absorption in the atmosphere and in clouds can be neglected in this spectral band. However, a correction for the atmospheric ozone absorption is required. The consideration of the anisotropy of the cloud reflectance is essential for the overall accuracy of the parameterization. This is the conversion of the measured bidirectional reflectance factor $R_T(\mu_o, \mu, \varphi)$ into the directional-hemispherical reflectance at the top of the atmosphere. The only data set published so far was derived from the ERB-Scanner measurements of Nimbus-7 (Taylor and Stowe, 1984). It contains anisotropy factors $f(\mu_o, \mu, \varphi)$ for eight different surfaces (low, medium, high clouds, ice clouds, land, ocean, snow, ice). Because they result from zonal averaged data, it is hazardous to apply them to individual clouds or cloud-free scenes. However, there is presently no alternative. The top-of-cloud reflectance $R(\mu_o)$ then is

$$R(\mu_o) = R_T(\mu_o, \mu, \varphi) \,/\, [f(\mu_o, \mu, \varphi) \cdot T_{03}(\mu_o) \cdot T_{03}(\overline{\mu, \varphi})] \tag{1}$$

with μ_o the cosine of the solar zenith angle, μ the cosine of the zenith angle of observation, φ the azimuth difference between sun and observation, $\overline{\mu, \varphi}$ the average value from all directions μ, φ, i.e. the diffuse transmittance of the ozone $T_{03}(\overline{\mu, \varphi})$. The quantity of interest now is not $R(\mu_o)$ but the reflectance $R_c(\mu_o)$ of the cloud only. The latter is related with $R(\mu_o)$ by (Chandrasekhar, 1950)

$$R(\mu_o) = R_c(\mu_o) + \frac{A_s T_c(\mu_o) T_c}{1 - A_s R_c} \tag{2}$$

A_s is the surface albedo, T_c the cloud transmittance either into the direction μ_o or diffuse, and R_c the bihemispherical reflectance of the cloud bottom which is set equal to R_c at the cloud top. Because absorption is negligible, T_c can be replaced by 1-R_c and $T_c(\mu_o)$ by 1-$R_c(\mu_o)$. If equation (2) is integrated with respect to μ_o, it can be solved for R_c if R_c is set equal to $2\int_0^1 R_c(\mu_o)\mu_o d\mu_o$. R can also be obtained from the Nimbus-7 ERB data (Taylor and Stowe, 1984) as an average value of $R(\mu_o)$: $R = R(\mu_o)/g(\mu_o)$ with roughly $0.8 \leqslant g \leqslant 1.2$. A_s can be approximated by the surface albedo of the nearest cloud-free pixel. The latter follows from $A_p = a + bA_s$ (Koepke and Kriebel, 1987), with A_p the planetary albedo of the cloud-free pixel obtained from the measured bidirectional reflectance factor and the anisotropy correction factor for, e.g., land after Taylor and Stowe (1984). a and b are path radiance and atmospheric transmittance. Averages over all surface types have been computed by Koepke (1988) for various solar elevations, atmospheric turbidities and water vapour contents. The complete equation for the cloud reflectance is

$$R_c(\mu_o) = \frac{R(\mu_o)[g(\mu_o)(1 - A_s) + A_s] - g(\mu_o)A_s}{g(\mu_o)(1 - 2A_s) + R(\mu_o)A_s} \tag{3}$$

$R(\mu_o)$ follows from $R_T(\mu_o, \mu, \varphi)$ according to equation (1). $R_c(\mu_o)$ is used in the parameterizations. It is related to the optical depth $\delta(\mu_o)$ of water clouds by (Stephens, 1978):

$$\delta(\mu_o) = \frac{R_c(\mu_o)}{1 - R_c(\mu_o)} \cdot \frac{\mu_o}{\beta(\mu_o)} , \tag{4}$$

Stephens has modified the backscattering coefficient $\beta(\mu_o)$ which allows the application of equation (4) which was originally obtained by Coakley and Chylek (1975) for optically thin layers, for thick clouds also. Optical depth δ is related to liquid water path w (Stephens, 1978) as

$$\log w = (\delta \cdot 0.5454)^{0.254} \tag{5}$$

This holds for all water clouds if an uncertainty of about $\pm$ 10 % is taken into account which results from neglecting the variability due to different droplet size distributions. The emissivity then is

$$\varepsilon = 1 - \exp(-a_0 \cdot w) \tag{6}$$

with $a_o = 0.13$ for upward and $a_o = 0.158$ for downward radiation.

Platt et al. (1980) have given a correction factor for the reflectance of ice clouds of 1.6 at medium solar elevations. If this correction is applied to the measured ice cloud reflectance, equation (4) can be used for ice clouds as well. The relation of reflectance with ice water path has been parameterized by Starr and Cox (1985). $\rho(\vartheta_o)$ is obtaind from $R_c(\mu_o)$ by applying the spectral correction after Welch et al. (1980). Then $\rho(60°)$ is obtained from

$$\rho(\vartheta_o) = (0.161 + 0.0117 \cdot \vartheta_o + 0.386 \cdot 10^{-4}\vartheta_o^2) \cdot \rho(60°) \tag{7}$$

$$+ (0.914 - 0.0152\vartheta_o)[\rho(60°)]^2 .$$

The upward emissivity then follows from

$$\rho(60°) = 0.557\varepsilon + 0.105\varepsilon^2 \tag{8}$$

and the ice water path from

$$\varepsilon = 1 - \exp(-\beta \cdot IWP) \tag{9}$$

with $\beta = 0.05\ m^2 g^{-1}$ as the 'effective upward broadband infrared mass absorption coefficient'. Starr and Cox give $\beta = 0.06$ at nighttime and $\beta = 0.07$ at noon for the 'downward' mass absorption coefficient, leading to

$$\varepsilon(\uparrow, \downarrow) = 1 - \exp[-\beta(\uparrow, \downarrow)IWP] . \tag{10}$$

5. VALIDATIONS

The assessment of the accuracy of the results is by far not yet finished. A conservative estimate gives about ± 50 % uncertainty in the liquid water content. First validations seem to support this estimate. Figure 2 shows vertical profiles of the liquid water content of stratus clouds obtained with an airborne Johnson-Williams liquid water probe (cf. Kriebel, 1989). The vertical integrals give 155 gm^{-2} (left) and 103 gm^{-2} (right). APOLLO derived LWP data of the areas containing the flight paths, measured about 30 minutes later than the airborne data, give 95 gm^{-2} and 69 gm^{-2} , respectively. This agreement is encouraging because it is roughly in the expected range of ± 50 % and it shows that horizontal inhomogeneitis do not affect the parameterization relations in a substantial way (Kriebel et al., 1989). Further, the accuracy of the Johnson-Williams probes themselves is believed to be ± 30 % (Strapp and Schemenauer, 1982; Kriebel et al., 1989). Therefore, a realistic accuracy assessment requires many comparisons of satellite data with airborne in-situ measurements. During the ARKTIS 88 campaign run in Spitzbergen in 1988, aircraft measurements of the cloud droplet distributions have been performed with Knollenberg PMS probes (Finger et al., 1989). Coincident satellite data have been recorded by means of a transportable NOAA HRPT station of DLR. A first comparison of satellite derived liquid water path of an arctic stratus cloud with simultaneous airborne PMS data was evaluated for the 24 May 1988 at 79.9 ° N and 4.9 ° E. In this case the APOLLO liquid water path was found to 14.6 gm^{-2} and the vertically integrated PMS-probe data yield 8.4 gm^{-2}. Again the airborne in-situ data are within a factor of 2 of the APOLLO data, however the sign of the deviation is opposite to the other two water cloud validations obtained so far. Possible reasons for this difference are a wrong anisotropy correction due to the low sun elevation in high latitudes, an ice contaminated sea surface introducing higher LWP data, and different sensitivities of the Johnson-Williams and the PMS probe. Anisotropy correction is not more than

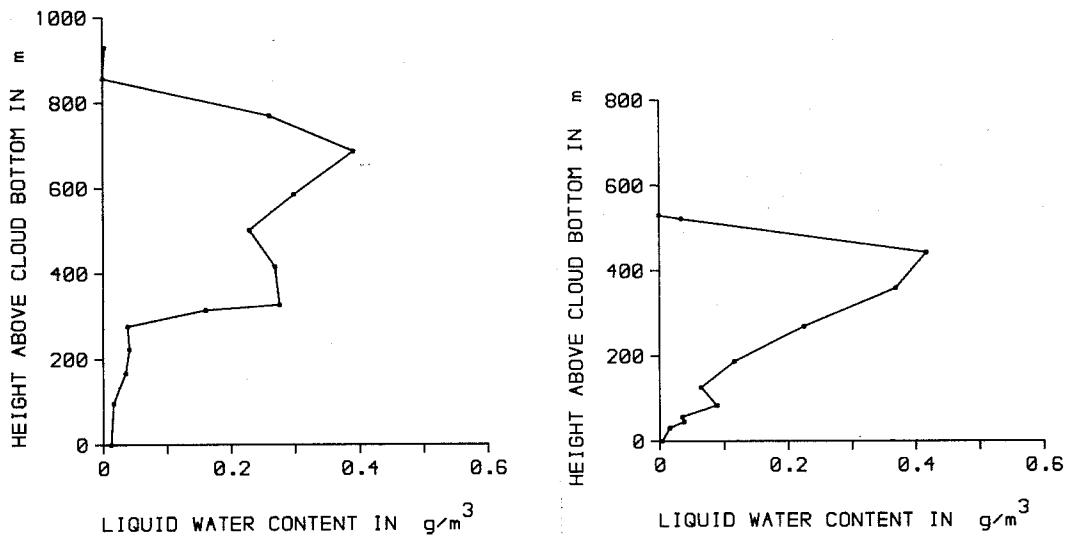

Figure 2: Liquid water content of stratus clouds measured with an airborne Johnson-Williams probe (Kriebel, 1989). The vertical integral, the liquid water path, amounts to 155 gm^{-2} (left) and 103 gm^{-2} (right). The corresponding results obtained with APOLLO are 95 gm^{-2} and 69 gm^{-2}, respectively.

20 % and cannot be the cause for the observed difference. Immediately after the aircraft descended below the cloud lower boundary, photographs have been taken which show a clean, ice-free ocean. According to many simultaneous measurements (e.g. Hoffmann, 1989), the differences in the measured LWC between Johnson-Williams probe and PMS FSSP have different signs. A possibility to explain this lies in the presumption that JW and FSSP give similar results with medium cloud drop sizes but differ up to a factor of 2 with small and large droplets, were JW probe gives higher values than the FSSP with small droplets ($< 30\ \mu m$) and lower values with large droplets ($> 60\ \mu m$). If this guess turns out to be true, it could explain most of the difference between the aircraft validation data obtained so far because they have been performed at stratus clouds which usually consist of small droplets.

A similar validation has been started with ice clouds. During the 'International Cirrus Experiment' (ICE) 1987, measurements of the backscattering coefficient of cirrus clouds have been performed with an upward directed Lidar system (Schmitz-Peiffer et al., 1989), from which the optical depth of the cirrus cloud has been estimated. NOAA-9 satellite data taken one hour before the aircraft data, have been processed with APOLLO and area average of the optical depth containing the aircraft flight path of about 0.8 was found. The Lidar measurements gave optical depths between 0.4 und 1.6 with an average around 0.7. Both systems seem to produce data in the same order of magnitude. How good the agreement really is, cannot be said presently.

6. FUTURE DEVELOPMENTS

The ways to a quantitative interpretation of satellite data presented here are based on a careful exploitation of a multispectral information. Their operational application is not very far developed, but parameters like the vegetation index, the surface temperature and the cloud coverage are increasingly required. If mesoscale models will be put into operation operationally, the requirement for high resolution data sets to help initializing such models will increase. Besides the cloud coverage, the liquid/ice water path of clouds is a possibly suitable quantity for this purpose.

This will be only possible if multispectral satellite data will be continuously available and the methods and parameterizations applied are improved and validated sufficiently. As far as one can see, all future imaging radiometers of the meteorological satellites will comprise at least those spectral channels realised in the AVHRR/2. This is true for the AVHRR/3 of the NOAA-K,L,M series which contains additionally (or alternatively to the 3.7 μm channel) a 1.6 μm channel, as well as for the 'Advanced Medium Resolution Imaging Radiometer' (AMRIR) proposed for the polar platform, and for the 'Visible and Infrared Imager' (VIRI) of the METEOSAT Second Generation System whose exact configuration is not yet defined but will very likely contain a 1.6 μm channel and two water vapour channels around 6.3 μm additionally to the AVHRR/2 channels (cf. Table 1). This means that algorithms using the AVHRR/2 channels can be applied to satellite data at least in the next 15-20 years. Certainly improvements are required of the algorithms presently in use and extensions which either make better use of the information already given (e.g. Pollinger and Wendling, 1984) or include pattern recognition techniques for cloud classification or take advantage of additional spectral channels. Finally it should be emphasized, that the quantitative evaluation of satellite data for operational purposes plays a key role in future satellite meteorology because only by such efforts sufficient use can be made from imaging radiometer data, similar to operational techniques in multispectral temperature sounding.

REFERENCES

Arking, A. and J.D. Childs, 1985: Retrieval of cloud cover parameters from multispectral satellite images. J. Clim. Appl. Meteor. 24, S. 322-333.

Brest, C. L. and W. B. Rossow, 1988: Radiometric Monitoring and calibration of NOAA AVHRR channel 1 data. Preprints of the International Radiation Symposium, Lille (France) 18-24 August 1988.

Chandrasekhar, S., 1950: Radiative Transfer. Oxford Clarendon Press.

Coakley, J. A. and P. Chylek, 1975: The two-stream approximation in radiative transfer: Including the angle of the incident radiation. J. Atmos. Sci. 32, S. 409-418.

Eyre, J. R., J. L. Brownscombe and R. J. Allam, 1984: Detection of fog at night using Advanced Very High Resolution Radiometer (AVHRR) imagery. Met. Mag. 113, S. 266-271.

Finger, J. E., H. Förster and P. Wendling, 1989: Observational Strategy of the DFVLR for the Arctic stratus cloud program. In: Field Phase Report ARKTIS 88, Hamburger Geophysikalische Einzelschriften, Ed. B. Brümmer, Reihe B, Heft 8.

Frouin, R. and C. GAUTIER, 1987: Calibration of NOAA-7 AVHRR, GOES-5 and GOES-6 VISSR/VAS solar channels. Remote Sens. Environ. 22, S. 73-101.

Gesell, G., 1989: An algorithm for snow and ice detection using AVHRR data: An extension to the APOLLO software package. Int. J. Remote Sensing 10, February Issue, in press.

Hoffmann, H.-E., 1989: The horizontal and vertical structures of cloud physical parameters. Extended abstract for conference preprint volume of Fifth WMO Scientific Conference on Weather Modification and Applied Cloud Physics Beijing, China, 8-12 May 1989.

Koepke, P. and K.T. Kriebel, 1987: Improvement in the shortwave cloud-free radiation budget accuracy. Part I: Numerical study including surface anisotropy. J. Clim. Appl. Meteor. 26, S. 374-395.

Koepke, P., 1988: Private Communication.

Kriebel, K.T., 1989: Cloud liquid water path derived from AVHRR data using APOLLO. Int. J. Remote Sensing, 10, April/May Issue (1989) in press.

Kriebel, K.T., R.W. Saunders and G. GESELL, 1989: Optical Properties of Clouds derived from fully cloudy AVHRR Pixels. Subm. Beitr. Phys. Atmos.

Lauritson, L., G. J. Nelson and F. W. Porto, 1979: Data extraction and calibration of TIROS-N/NOAA Radiometers. NOAA Technical Memorandum NESS 107, US Dept. of Commerce, NOAA/NESS.

Liljas, E., 1984: Processed satellite imageries for operational forecasting. Swedish Meteorological and Hydrological Institute, Swedish Space Corporation.

Liljas, E., 1988: Effective weather monitoring with METEOSAT Second Generation - Ideas stemming from experience of NOAA satellites. Proc. 7. METEOSAT Scientific Users Meeting, Madrid, 27-30 September (1988) EUMETSAT, Darmstadt, FRG, Ed.

Platt, C. M. R., D. W. Reynolds and N. L, ABSHIRE, 1980: Satellite and Lidar observations of the albedo, emittance and optical depth of Cirrus compared to model calculations. Mon. Wea. Rev. 108, S. 195-204.

Pollinger, W. and P. Wendling, 1984: A Bispectral Method for the Height Determination of Optically Thin Ice Clouds. Beitr. Phys. Atm. 57, No. 2, S. 269-281.

Price, J. B., 1987: Calibration of satellite radiometers and comparison of vegetation indices. Remote Sens. Environ. 21, S. 15-27.

Rao, C. R. N., 1987: Pre-launch calibration of channels 1 and 2 of the Advanced Very High Resolution Radiometer. NOAA Technical Report NESDIS 36, October (1987).

Raschke, E., H. Jacobs, H. J. Lutz and U. Steffens, 1987: Cloud analysis of AVHRR data measured over polar regions. In: Report of the ISCCP Workshop on Cloud Algorithms in the Polar Regions (Tokyo, 19-21 August 1986). WCP 131, WMO/TD-No. 170, March 1987, World Meteorological Organisation (1987) Geneva, CH.

Ruff, I. and A. Gruber, 1983: Multispectral identification of clouds and earth surfaces using AVHRR radiometer data. Preprints 5. Conf. Atm. Radiation, October 31 - November 4 (1983) Baltimore, Md., AMS, Ed., Boston, Mass., USA

Saunders, R.W., 1986: An automated scheme for the removal of cloud contamination from AVHRR radiances over western Europe. Int. J. Remote Sensing, 7, No.7, S. 867-886

Saunders, R.W., 1988: Cloud top temperature/height: A high resolution imagery product from AVHRR data. Met. Mag. 117, S. 211-221.

Saunders, R.W. and K.T. Kriebel, 1988: An improved method for detecting clear sky and cloudy radiances from AVHRR data. Int. J. Remote Sensing, 9, No.1, S. 123-150.

Schmitz-Peiffer, A., W. Renger and P. Mörl, 1989: Fernerkundung von Cirruswolken mit einem flugzeuggetragenen Lidarsystem. Submitted to Ann. Met. (NF), 26.

Starr, D. O'C. and S. K. Cox, 1985: Cirrus clouds. Part I: A cirrus cloud model. J. Atmos. Sci. 42, S. 2663-2681.

Stephens, G.L., 1978: Radiation profiles in extended water clouds II: Parameterization schemes. J. Atmos. Sci. 35, S. 2123-2132.

Taylor, V. R. and L.L. Stowe, 1984: Atlas of reflectance patterns for uniform earth and cloud surfaces (NIMBUS-7 ERB 61 days). NOAA Technical Report NESDIS 10.

Welch, R. M., S. K. Cox and J. M. Davis, 1980: Solar radiation and clouds. Meteorological Monographs 17, No. 39, May 1980, AMS Ed., Boston, MA, USA.

WMO, 1984: The International Satellite Cloud Climatology Project (ISCCP): Cloud analysis algorithm intercomparison. WCP-73, March (1984) World Meteorological Organisation, Geneva, CH.